The Study of the Effect of Mechanical and Heat Treatment on the Crystal Texture of Cold Drawn Seamless Tubes

Pavel Kejzlar[1], Ondřej Seibert[1], Zuzana Andršová[1], Peter Burik[2]
[1]Technical University of Liberec. Studentska 1402/2, 461 17, Liberec. Czech Republic. E-mail: pavel.kejzlar@tul.cz, zuzana.andrsova1@tul.cz, ondrej.seibert@tul.cz
[2]ŽP VVC, s.r.o. Kolkáreň 35, 976 81 Podbrezová. Slovakia. E-mail: burik@zelpo.sk

Seamless tubes are the strongest amongst all tubes types and have a homogeneous structure throughout their length. They are typically manufactured by cold drawing where strong grain deformation takes place. EBSD was used to evaluate the changes of grain structure and texture connected with tubes manufacturing from the initial state over the cold drawing with a stationary plug to subsequent recrystallization annealing.

Keywords: Structure, Texture, Grain, EBSD, Drawing, Deformation

1 Introduction

There are several possibilities for manufacturing of tubes. The first possibility includes welded tubes where the weld can be longitudinal or into a helix. Shaped tubes are manufactured by rolling from the metal sheet by molding to the desired shape. The last method contains manufacturing of seamless tubes. The process of seamless tubes manufacturing is well described e.g. in [1].

To achieve closer wall thickness and diameter tolerances, an improvement in surface finish and some mechanical properties a considerable proportion of seamless tubes undergo subsequent cold forming. Though the cold forming process it is also possible to expand the product portfolio toward the lower outer diameters and wall thickness scales. Cold-formed seamless tubes benefit from their very good surface finish, close dimensional control, homogeneous structure over their length and their superior mechanical properties, therefore they are widely used for piping systems.

In the tube cold drawing manufacturing are dominating three processes: hollow drawing, drawing over a mandrel and stationary or floating plug drawing (***Fig. 1***). [1]

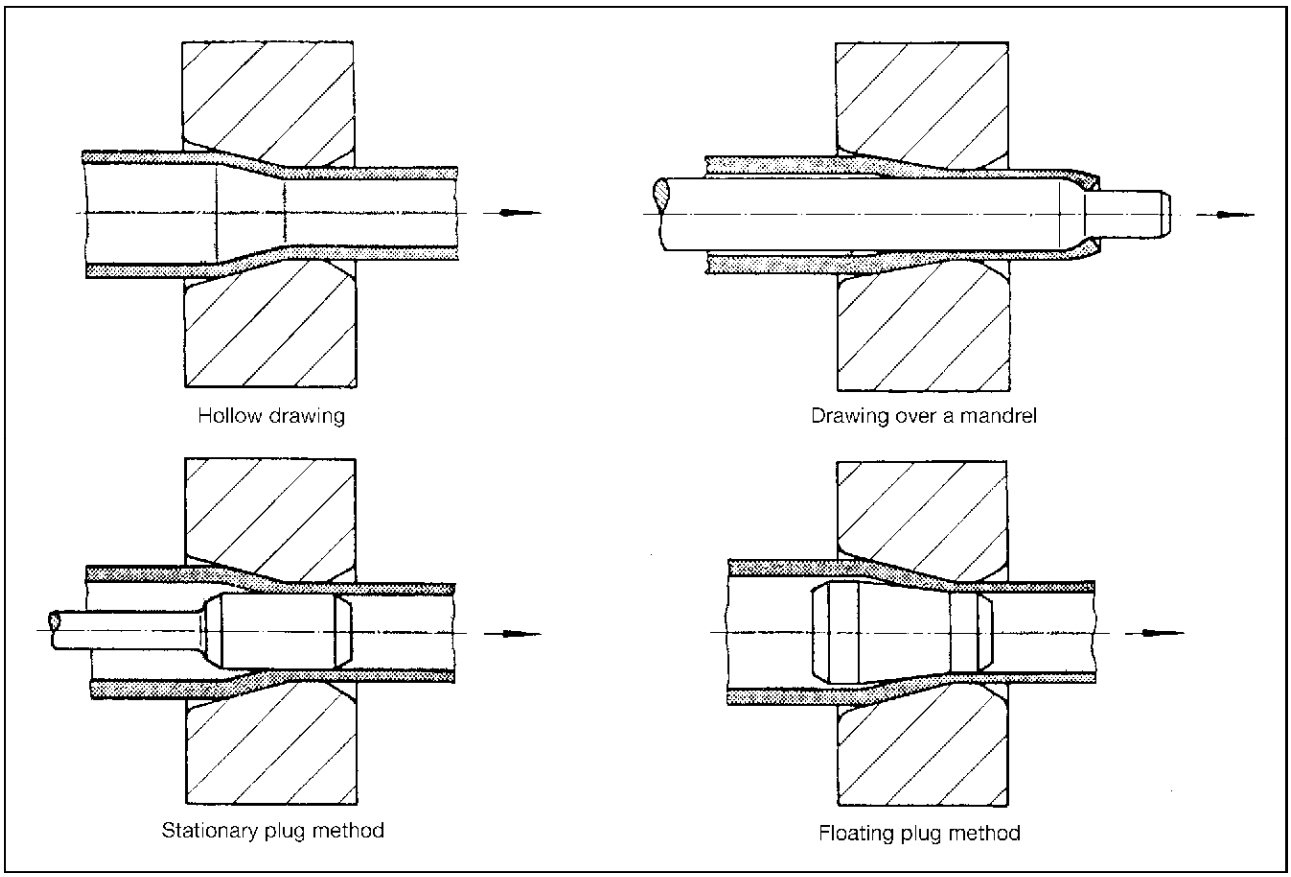

Fig. 1 *The most used methods for tube cold drawing. [1]*

In the hollow drawing, only the outer diameter is reduced while the internal diameter undergoes only negligible changes. In the drawing over the mandrel, the tube is pulled over the die with a mandrel bar inserted into the tube. This method allows to achieve the highest diameter reduction per draw from the above-mentioned methods, but the length of the tube is limited by the length of the inserted mandrel bar. The plug drawing uses a plug, which is either fixed to a mandrel bar or so-called floating plug. The die and inserted plug act together reducing both – tube's outer diameter and its thickness within close tolerances. In addition, both surfaces (inner and outer) are smoothed and polished. [1-3]

The low temperature during the cold drawing process doesn't enable dynamic recrystallization and thus occurs the material hardening due to the accumulation of dislocations. During the forming process, individual grains are elongated in the direction of the main deformation. Too high level of deformation and hardening is connected with a depletion of material plasticity and the risk of defects, and therefore recrystallization annealing is required. During the annealing, the new deformation-free equiaxial grains are formed and the material is capable of being further deformed. [1,4,5].

The EBSD analysis is a highly accurate analytical method which uses an elastic interaction of electrons with crystal lattice. The interaction produces backscattered electrons which create a pattern (so-called Kikuchi's bands) which can be identified with a fluorescent screen of EBSD detectors. The patterns carry information about the crystal structure and lattice rotation at any region of the sample and therefore can be used for detailed study of the grain size and orientation, structure, and deformation structure. [6-9] These output data could help to analyze deformation degree of material after individual drawing steps and can be used for optimization of the drawing process.

2 Experimental

The tube was manufactured from E355 ferritic steel grade (according to CSN 41 1353; EN SPT360); its composition is in ***Tab. 1***.

Tab. 1 *Material composition according to standard CSN 41 1353*

Element	C	Ni	Mn	Mo	Cr	Fe
Concentration [wt. %]	≤ 0.09	≤ 0.06	≤ 0.42	≤ 0.02	≤ 0.06	Bal.

The input feedstock (a tube Ø 31,8 x 2,6 mm) was normalized after previous hot rolling. The conditions for normalization in the continuous furnace were: T = 900-930 °C / 20 min (corresponds to a speed of 35 m/s through the furnace). The material was further treated by a stationary plug drawing in two steps. In the first step, the outer diameter was reduced from 31.8 to 28 mm and the inserted plug's diameter was 24 mm (wall thickness 2 mm); in the second step the outer diameter was reduced to 25 mm and the diameter of the plug was 22 mm (wall thickness 1.5 mm). The third examined state includes the sample which has been recrystallized after the second pass. The recrystallization took place in the continuous furnace at 850 °C / 20 min. The summary of samples used for the analysis is in ***Tab. 2***.

Tab. 2 *Samples description*

Sample	State/treatment	Sample outer diameter [mm]	Wall thickness [mm]	Thickness reduction [%]
N	Input hollow tube; normalized after hot rolling	31.8	2.6	-
D1	After cold drawing; 1st step	28.0	2.0	31.5
D2	After cold drawing; 2nd step	25.0	1.5	32.2
R	After recrystallization	25.0	1.5	-

The samples for metallographic characterization were hot fixed into a polymeric resin and subsequently grinded and polished. Mechanical-chemical polishing using colloidal silica (OP-S Struers) took place as a final step. The microstructure was evaluated using light optical microscope GX51.

EBSD analysis of samples after mechanical and heat treatment were performed on Zeiss Ultra Plus scanning electron microscope fitted with an Oxford NordlysNano detector. EBSD data were acquired at accelerating voltage of 20 kV, sample tilt 70°. The EBSD step size was 1 μm. The EBSD data were acquired using software AZtec and processed in Channel5 - Tango Maps.

3 Results and discussion

The structure (***Fig. 2***) is predominantly ferritic with a minor fraction of pearlite. The grains are equiaxial in the initial state (***Fig. 2A,B*** after normalization annealing). In the longitudinal section there is visible banding coming from the manufacturing process (hot rolling and piercing of hollow tube). The banding remains also after the drawing and subsequent annealing. After cold drawing (***Fig. 2C,E***) there is visible grain elongation, which is more perceptible after the second step. The material consisting of equiaxed grains was obtained through the recrystallization annealing (***Fig. 2G,H***). The average grain diameter obtained from image analysis in ***Tab. 3***. Both steps of cold drawing led to a decrease in the average grain size, in both cases the relative grain size reduction achieved approx. 30 %. The subsequent recrystallization led to a 7 % increase in the grain average diameter compared to the initial state before the cold drawing. The increase of the grain size due to the heat treatment is an undesirable effect indicating that the material deformation degree or the heat treatment parameters were not optimal.

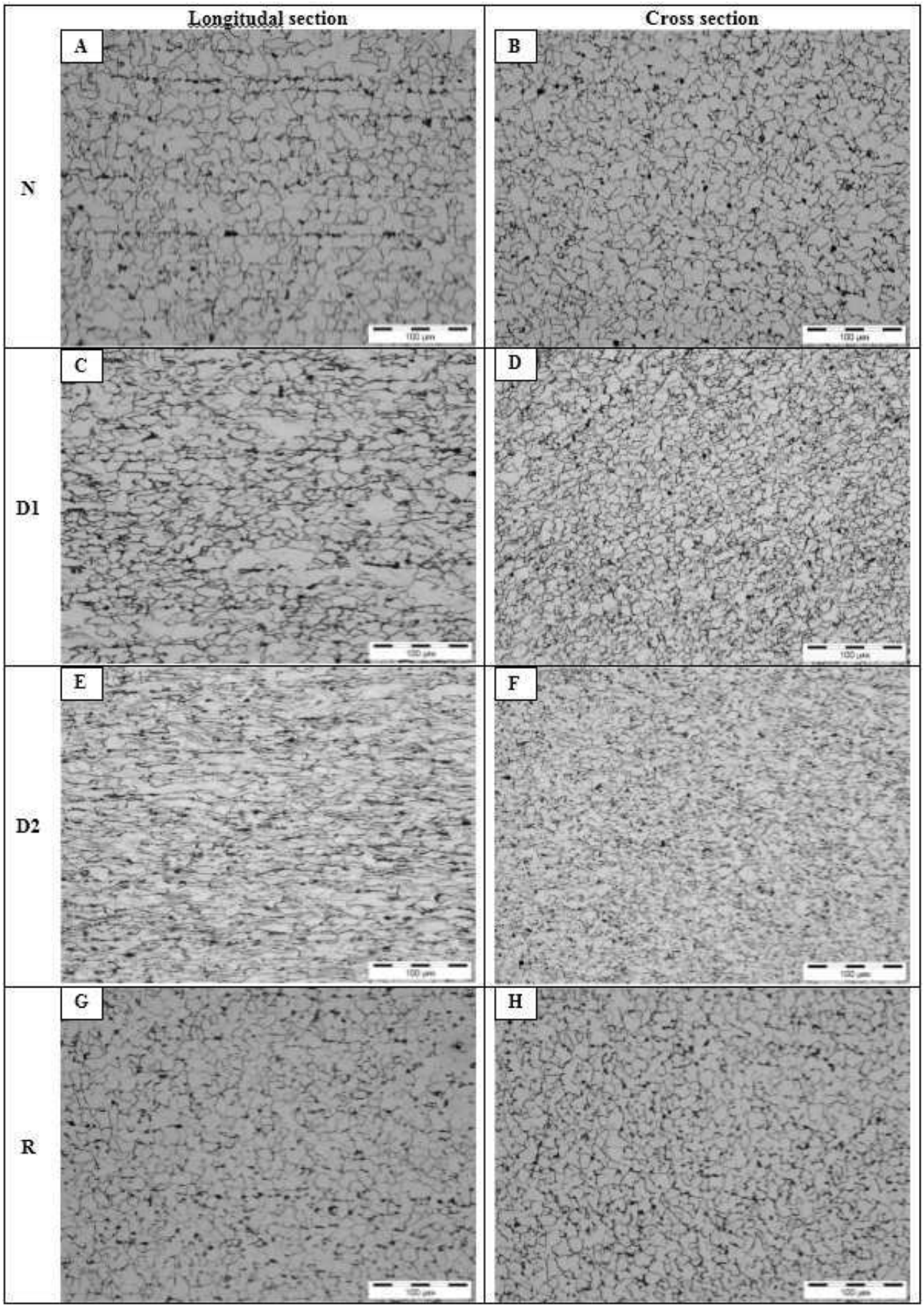

Fig. 2 *The structures seen by the optical microscope in longitudinal and in cross sections*

Tab. 3 *Average grain diameter (from optical microscopy)*

Sample	Grain diameter [μm]
NA	7.5 ± 0.4
D1	5.4 ± 0.4
D2	3.8 ± 0.1
RA	8.0 ± 0.5

The data for construction of EBSD maps were taken from longitudinal sections as marked in ***Fig. 3A***; the length of EBSD steps during mapping was 1 μm. EBSD maps show the longitudinal section of the tube wall (outer diameter is left; inner is on the right side). The main sample directions with respect to the way of the cut preparation are obvious from ***Fig. 3A***, where RD means rolling direction (tube length), ND normal direction (wall thickness) and TD transverse direction (tangent to the tube diameter). Inverse pole figure maps were used for the illustration of preferred grain orientation; the colour coding of elementary crystal cell orientations is in ***Fig. 3B***.

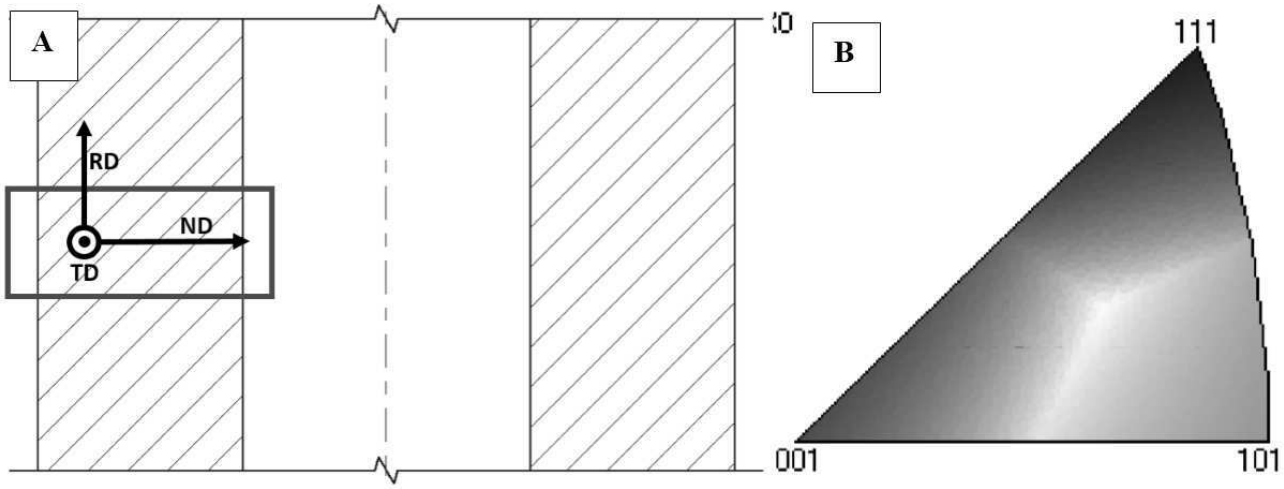

Fig. 3 *A) A schema of the EBSD scans position on the tube section including the main sample directions; B) colour coding for EBSD IPF maps.*

Figures 4-7 show IPF maps of the samples after individual technological steps (initial state; after 1st and 2nd step of cold drawing and after recrystallization). The orientation of individual grains is marked by colours, the colours indicate which crystal direction is parallel to respective sample direction, e.g. the dominant green colour in sample's D2 RD IPF map indicates that most of the grains are oriented with its <110> parallel to the rolling direction.

The grain coarsening near the outer diameter is obvious in the initial state (***Fig. 4)***. This was probably caused by surface decarburization and dynamic recrystallization during the previous hot rolling process (manufacturing of hollow tube).

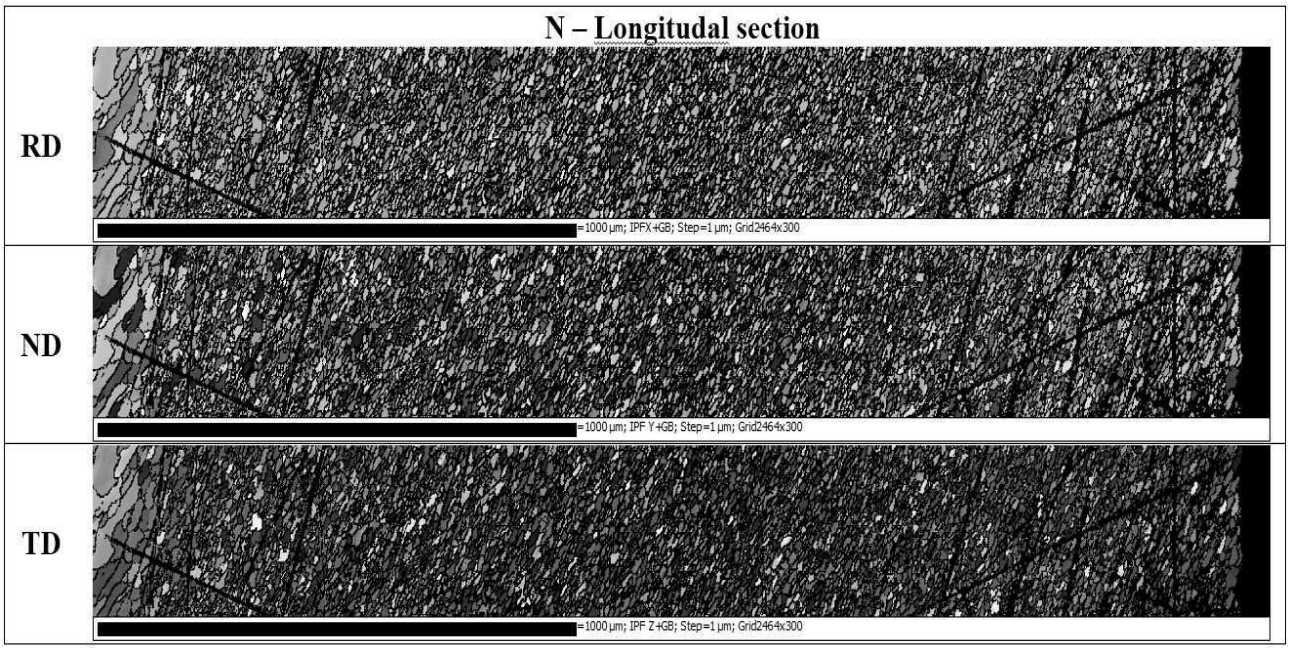

Fig. 4 *IPF maps for sample* ***N***

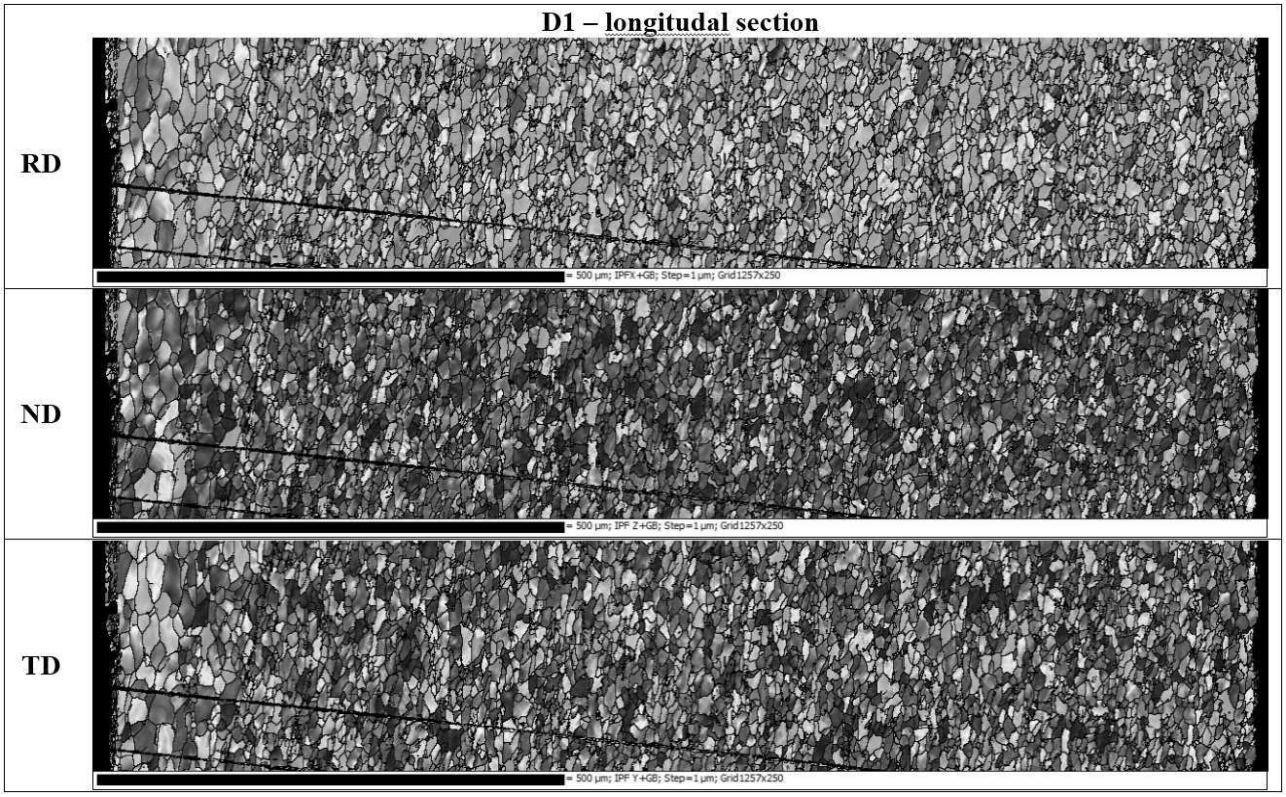

Fig. 5 *IFP maps for sample* ***D1*** *(after the 1st step of drawing)*

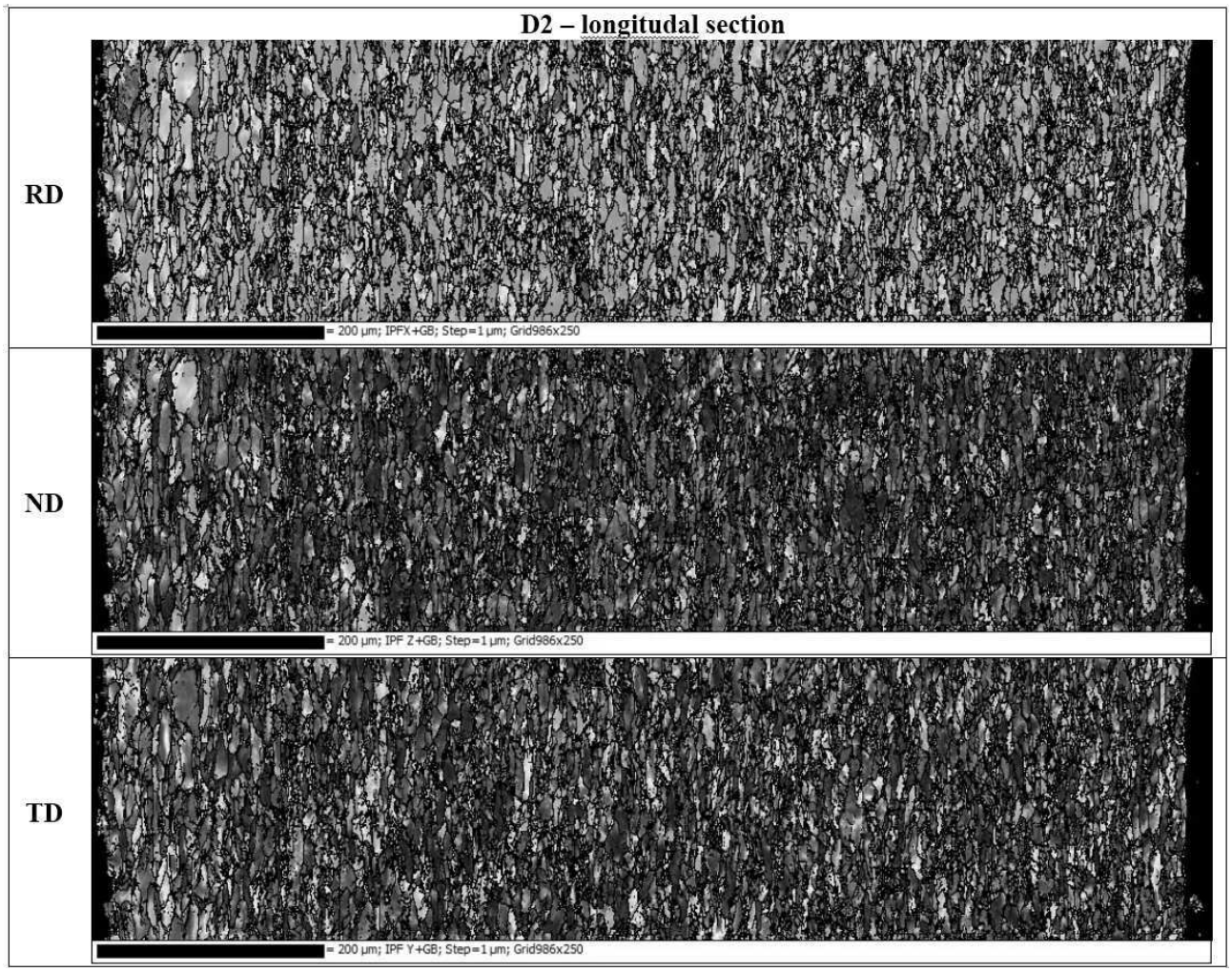

Fig. 6 *IPF maps for sample* ***D2*** *(after two steps of drawing)*

After the first step of drawing, we can observe slightly elongated grain parallel to the rolling direction. The grains are coarsened near the outer surface. We can observe a deformation inside large grains – it manifests itself as colour variation inside individual grains. This is caused by the presence of low-angle boundaries. The drawing process caused the change in preferred orientation of grains. In the rolling direction dominates the green colour. The green colour means, that the most of grains are oriented with their <110> parallel to the rolling direction. The crystal plane {110} in the body-centered cubic (BCC) lattice of ferrite is the most densely occupied by atoms and therefore the deformation occurs by sliding in this plane. In addition, the BCC lattice responds to pressure stress by rotating the body diagonal <111> parallel to the direction of applied stress.

A similar effect is obvious after the second step of cold drawing (***Fig. 6***). The grain is significantly elongated. The high deformation led to grain refinement. Colour variation inside grains marks high density of subgrain boundaries connected with a high degree of deformation. Predominant green colour in RD and blue colour in ND and TD corresponds to the fact, that the body-centered cubic of ferrite orients itself according to applied stress; <110> parallel to tensile stress and <111> parallel to compressive stress.

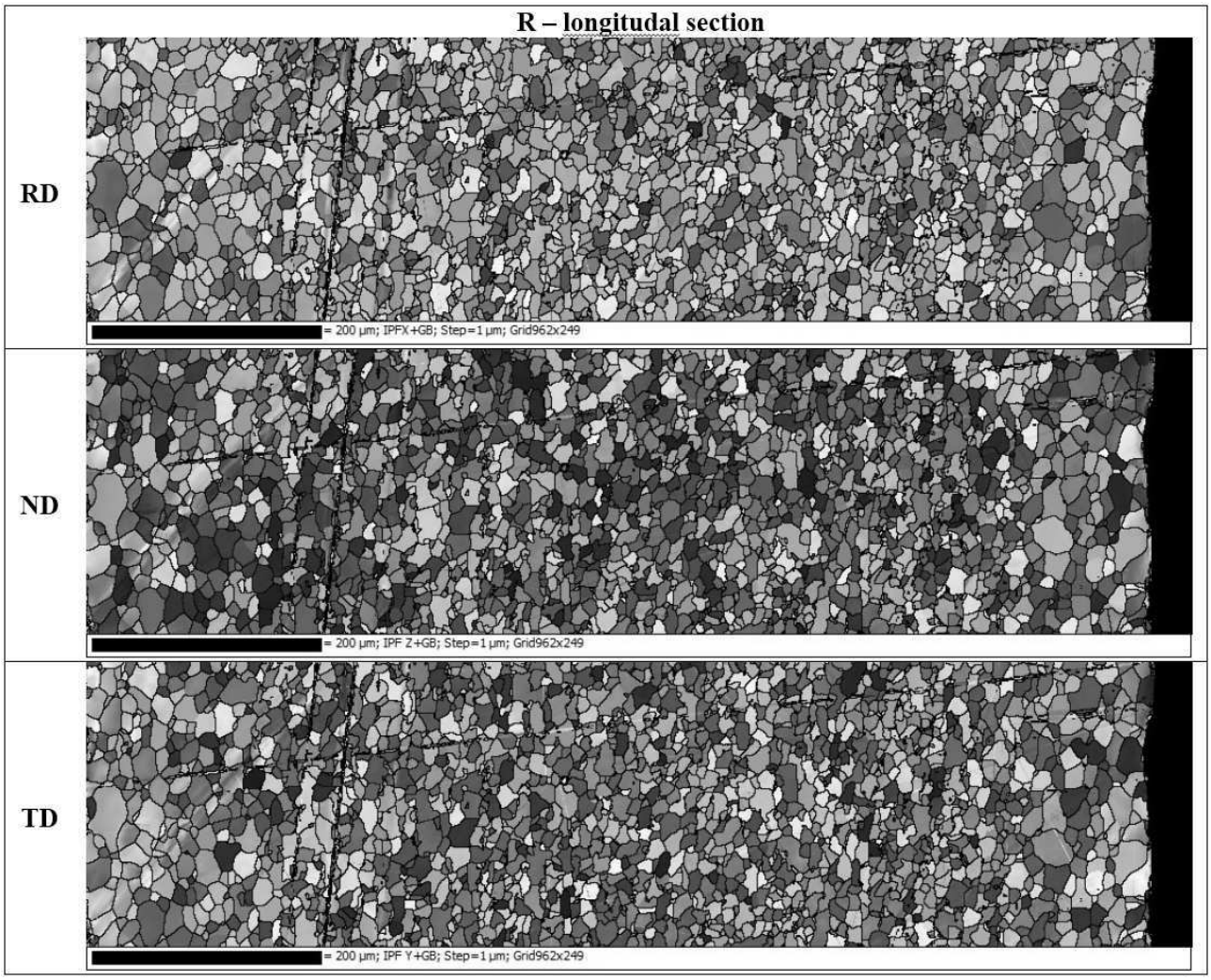

Fig. 7 *IPF maps of sample* ***R*** *after the recrystallization annealing.*

The grains are equiaxial and deformation-free after the recrystallization (***Fig. 7***). The absence of colour shading inside the grains indicates that there is no internal residual stress in the material. Even after recrystallization, a certain inheritance of the deformation texture is evident (visible as predominant colouring for individual sample directions). We can observe significant grain coarsening near both surfaces, outer and inner. This could be related to the surface decarburization during the heat treatment.

The inverse pole figures in ***Fig. 8*** show the evolution of the deformation structure. In the initial state, there is a strong dominance of <001> || to TD and <110> || to RD as a result of the previous deformation during the hot rolling. The process of cold drawing is connected to the evolution of <111> || to ND and TD as a result of applied compressive stress and strong <110> || to RD orientation caused by tensile deformation. The recrystallization annealing led to alleviation of the deformation texture and re-appearance of <001> in all directions (ND, TD, and RD).

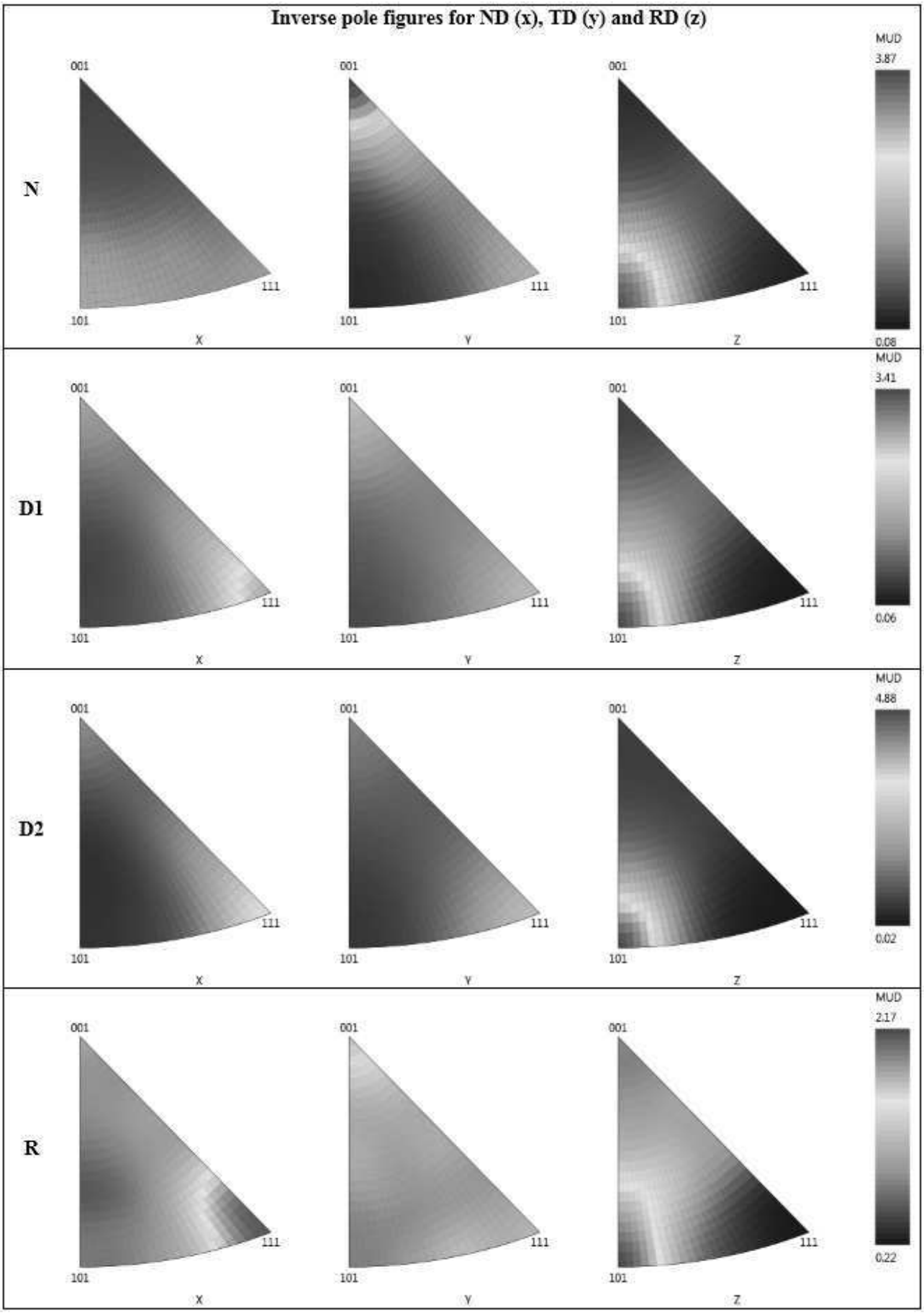

Fig. 8 *Inverse pole figures showing the evolution of texture after cold drawing and subsequent recrystallization.*

4 Conclusion

The grains structure and deformation texture were studied in different degrees of the cold-drawn seamless tubes manufacturing process. The structural and textural changes observed through the light optical microscopy and EBSD analysis were documented and described for all investigated states – in the initial state (hot rolled hollow tube after normalization); after the first and second step of cold drawing and after subsequent recrystallization annealing. Obtained data served as a valuable basis for the optimization of technological processes of production.

Acknowledgement

This publication was written at the Technical University of Liberec as a part of project "The study and evaluation of the material's structure and properties" with the support of the Specific University Research Grant, as provided by the Ministry of Education, Youth and Sports of the Czech Republic in the year 2018.

References

[1] BRESING, K.H., SOMMER, B. (2008). *Steel Tube and Pipe Manufacturing Process*. Salzgitter Mannersmann Rohrenwerke.

[2] LOHARKAR, P. K., PRADHAN M. K. (2017) Modeling and Analysis of Cold Drawing Process. In: *Handbook of Research on Manufacturing Process Modeling and Optimization Strategies* (R. Das, M. Pradhan, (Ed.)), pp. 40-53 IGI Global, Advances in Logistics, Operations, and Management Science. ISBN 9781522524403.

[3] LINARDON, C. (2013). Precision tube drawing for biomedical applications : Theoretical, Numerical and Experimental study. Université de Grenoble.

[4] RAJI, N. A., OLUWOLE O. O. (2011). Influence of Degree of Cold-Drawing on the Mechanical Properties of Low Carbon Steel. In: *Materials Sciences and Applications*, Vol. 02, No.11, pp. 1556-1563. ISSN 2153-117X.

[5] BELYAKOV, A, et. al. (2004). Microstructure Evolution in Ferritic Stainless Steels during Large Strain Deformation. In: *MATERIALS TRANSACTIONS*, Vol. 45, No.9, pp. 2812-2821. ISSN 1345-9678.

[6] SCHWARTZ, A. J. (2009). *Electron backscatter diffraction in materials science*. 2nd ed. New York: Springer. ISBN 978-0-387-88136-2.

[7] ADAMS, B. L., KALIDINDI, S. R., FULLWOOD D. T. (2013). Electron Backscatter Diffraction Microscopy and Basic Stereology. In: *Microstructure Sensitive Design for Performance Optimization*. Elsevier, pp. 341-371. ISBN 9780123969897.

[8] KEJZLAR, P., MACHUTA, J., NOVÁ, I. (2017). Comparison of the structure of CuZn40MnAl alloy casted into sand and metal moulds. In: *Manufacturing Technology*. Univerzita J. E. Purkyně, Vol.17, No.1, pp. 44-48. ISSN 12132489.

[9] TREGLER, M., et. al. (2016). The study of deformation behaviour of DC06 deep drawing steel. In: *Manufacturing Technology*. Vol. 16, No. 1, pp. 284-289. ISSN 12132489.

10.21062/ujep/142.2018/a/1213-2489/MT/18/4/585